28. Jonker, R. R., Meulemans, J. T., Dubelaar, G. B. J., Wilkins, M. F. & Ringelberg, J. Flow cytometry: a powerful tool in analysis of biomass distributions in phytoplankton. *Water Sci. Technol.* **32,** 177–182 (1995).

Acknowledgements We thank M. Staal for his contribution to the isolation of the Baltic Sea picocyanobacteria, C. Sigon for support during the competition experiments, B. Sommeijer for advice on efficient numerical techniques, and O. Béjà for comments on the manuscript. The research of M.S. and J.H. was supported by the Earth and Life Sciences Foundation (ALW), which is subsidized by the Netherlands Organisation for Scientific Research (NWO).

Competing interests statement The authors declare that they have no competing financial interests.

Correspondence and requests for materials should be addressed to J.H. (jef.huisman@science.uva.nl).

Baf60c is essential for function of BAF chromatin remodelling complexes in heart development

Heiko Lickert[1]*, Jun K. Takeuchi[2,3]*, Ingo von Both[1], Johnathon R. Walls[4,5], Fionnuala McAuliffe[1,6], S. Lee Adamson[1,3,7], R. Mark Henkelman[4,5], Jeffrey L. Wrana[1,8], Janet Rossant[1,8] & Benoit G. Bruneau[2,3,8]

[1]*Samuel Lunenfeld Research Institute, Mount Sinai Hospital, 600 University Avenue, Toronto, Ontario M5G 1X5, Canada*
[2]*Cardiovascular Research and Developmental Biology,* [4]*Mouse Imaging Centre, The Hospital for Sick Children, 555 University Avenue, Toronto, Ontario M5G 1X8, Canada*
[3]*Heart and Stroke/Richard Lewar Centre of Excellence,* [5]*Department of Medical Biophysics,* [8]*Department of Molecular and Medical Genetics, University of Toronto, Toronto, Ontario M5S 1A8, Canada*
[6]*University College Dublin, Department of Obstetrics & Gynaecology, National Maternity Hospital, Holles Street, Dublin 2, Ireland*
[7]*Department of Obstetrics and Gynecology, University of Toronto, Toronto, Ontario M5G 1L4, Canada*

* These authors contributed equally to this work

Tissue-specific transcription factors regulate several important aspects of embryonic development. They must function in the context of DNA assembled into the higher-order structure of chromatin. Enzymatic complexes such as the Swi/Snf-like BAF complexes remodel chromatin to allow the transcriptional machinery access to gene regulatory elements[1,2]. Here we show that *Smarcd3*, encoding Baf60c, a subunit of the BAF complexes, is expressed specifically in the heart and somites in the early mouse embryo. *Smarcd3* silencing by RNA interference in mouse embryos derived from embryonic stem cells causes defects in heart morphogenesis that reflect impaired expansion of the anterior/secondary heart field, and also results in abnormal cardiac and skeletal muscle differentiation. An intermediate reduction in *Smarcd3* expression leads to defects in outflow tract remodelling reminiscent of human congenital heart defects. Baf60c overexpressed in cell culture can mediate interactions between cardiac transcription factors and the BAF complex ATPase Brg1, thereby potentiating the activation of target genes. These results reveal tissue-specific and dose-dependent roles for Baf60c in recruiting BAF chromatin remodelling complexes to heart-specific enhancers, providing a novel mechanism to ensure transcriptional regulation during organogenesis.

In a screen for targets of Wnt signalling (H.L., B. Cox, I.v.B., L. Attisano, J.L.W., M. M. Taketo, R. Kemler, J.R., unpublished work) we identified *Smarcd3*, which encodes Baf60c, a 60-kDa subunit of the BAF complexes[3]. *Smarcd3* mRNA and Baf60c protein are initially restricted to the developing heart, as early as embryonic day 7.5 (E7.5) (Fig. 1a–g). In the looping heart tube (E8.5–E9.0), *Smarcd3* expression is more pronounced at the poles of the heart, which will give rise to the outflow tract anteriorly and to the atria posteriorly (Supplementary Fig. 1). *Smarcd3* is also expressed

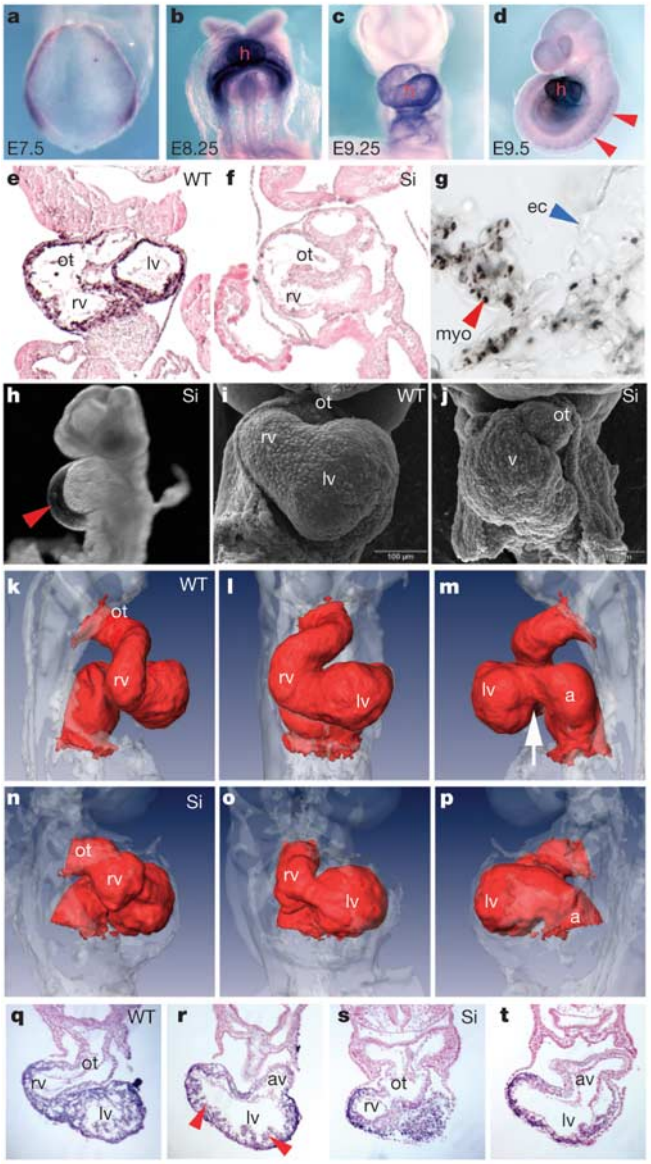

Figure 1 Baf60c is required for heart formation. **a**–**d**, *Smarcd3* is restricted to heart (h) at E7.75 (**a**), E8.25 (**b**) and E9.25 (**c**), and somites at E9.5 (arrowheads in **d**). **e**–**g**, Baf60c immunohistochemistry (brown) in E9.5 wild-type (WT; **e**, **g**) and *Smarcd3* knockdown (Si; **f**) embryos. Magnifications: ×10 (**e**, **f**), ×40 (**g**). **g**, Baf60c immunostaining in nuclei of myocardial cells (myo) but not endocardial cells (ec). **h**, Pericardial oedema in E8.75 *Smarcd3* knockdown embryo (arrowhead). **i**, **j**, Scanning electron micrographs of WT (**i**) and *Smarcd3* knockdown (Si; **j**) embryos at E8.75; a single ventricle (v) is apparent in the Si embryo. WT embryos have left ventricular (lv) and right ventricular (rv) chambers. **k**–**p**, Rendered OPT of E9.5 embryos viewed from the right (**k**, **n**), front (**l**, **o**), and left (**m**, **p**). The heart is red and the rest of the embryo is translucent. **k**–**m**, WT embryo. **n**–**p**, *Smarcd3* knockdown embryo, showing shortened outflow tract (ot), hypoplastic right ventricle (rv) and atrium (a), lack of atrio-ventricular canal (compare with **m**, arrow). **q**–**t**, Histology of E9.5 embryos stained by *in situ* hybridization with *Myl2* (blue). **q**, **r**, WT embryo; arrowheads show trabeculae. **s**, **t**, *Smarcd3* knockdown embryo. Note shortened outflow tract and lack of trabeculae (WT: arrowheads in **r**).

from E9.5 onwards in myotome of somites, dorsal neural tube, and limb bud mesenchyme (Fig. 1d; Supplementary Figs 1 and 2)[3,4]. In contrast, expression of the related genes *Smarcd1* and *Smarcd2* was not observed in the heart at these stages (Supplementary Fig. 2).

To address the role of *Smarcd3 in vivo*, we employed embryonic stem (ES)-cell-mediated transgenic RNA interference (RNAi)[5]. Three *Smarcd3* 'knockdown' ES cell clones with less than 15% wild-type mRNA amounts after cardiomyocyte differentiation (Supplementary Fig. 3; siSmarcd3-A#1, siSmarcd3-B#2 and siSmarcd-B#7) were used in tetraploid aggregations to generate entirely ES-cell-derived embryos[5]. Baf60c protein was greatly reduced in the knockdown embryos (by 96% in siSmarcd3-A#1), whereas other Baf proteins were not significantly affected (Fig. 1e, f; Supplementary Fig. 3). Cardiac malformations in all three lines were comparable (Fig. 1h–t), causing lethality at E10.0–E11.0. At E8.75, hearts of *Smarcd3* knockdown embryos had a hypoplastic atrium, and a single ventricle connected to an abnormal outflow tract; the myocardial wall of the heart appeared rougher than wild-type hearts (Fig. 1i, j). At E9.5, *Smarcd3* knockdown embryos had a shortened outflow tract, connected to a hypoplastic right ventricle (RV), which was connected to the left ventricle (LV) by an abnormal constriction (Fig. 1k–t, Supplementary Movie). Other phenotypes included failure of forebrain closure (Fig. 1h) and disorganized somites (Supplementary Fig. 5).

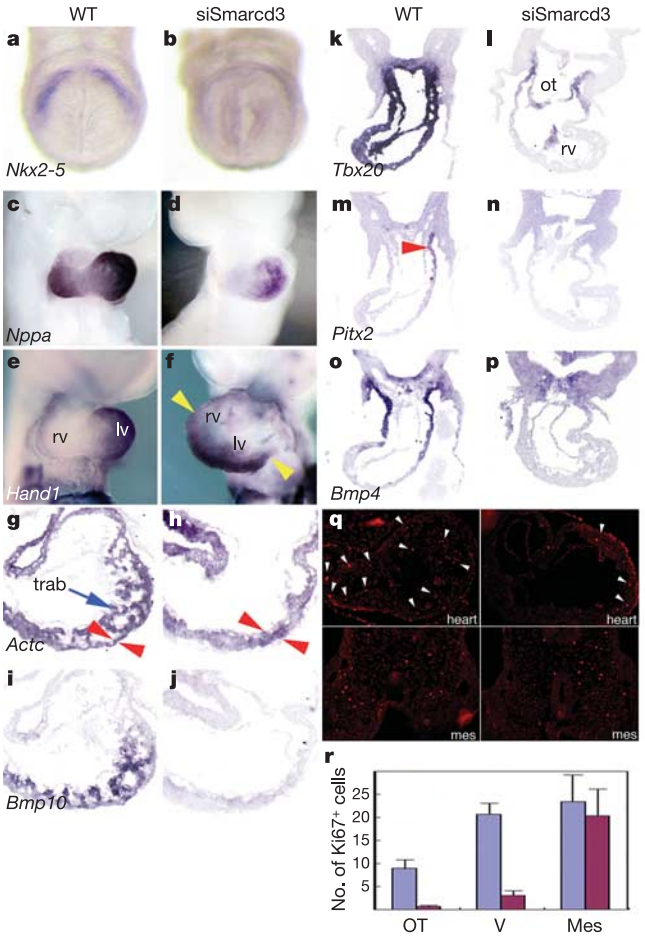

Figure 2 Cardiac gene expression in wild-type (WT) and *Smarcd3* knockdown (siSmarcd3) embryos. **a**, **b**, Decreased expression of *Nkx2-5* at E7.75 in siSmarcd3 embryos. **c**, **d**, Decreased expression of *Nppa* in siSmarcd3 embryos at E8.75. **e**, **f**, Expanded domain of *Hand1* expression in siSmarcd3 at E8.5 (distance between arrowheads). **g**, **h**, *Actc* staining shows lack of trabeculations (trab) and thicker myocardium (distance between arrowheads) in siSmarcd3 hearts. **i**, **j**, *Bmp10* expression is absent from siSmarcd3 hearts. **k**, **l**, *Tbx20* expression is reduced in the outflow tract (ot) and ventricles (v) of E8.75 siSmarcd3 hearts. **m**, **n**, *Pitx2* expression on the left side of the outflow tract (arrowhead in **m**) is absent from E8.75 siSmarcd3 hearts (**n**). **o**, **p**, *Bmp4* expression in the outflow tract is undetectable in E8.75 siSmarcd3 embryos. **q**, Ki67 staining of heart (top panels) or body mesenchyme (lower panels) shows decreased proliferation in SiSmarcd3 heart. Arrowheads show Ki67-positive nuclei in the heart. **r**, Quantification of Ki67 immunostaining ($n = 3$). OT, outflow tract; V, ventricles; Mes, mesenchyme; blue bars, wild type; red bars, siSmarcd3. Error bars indicate s.e.m.

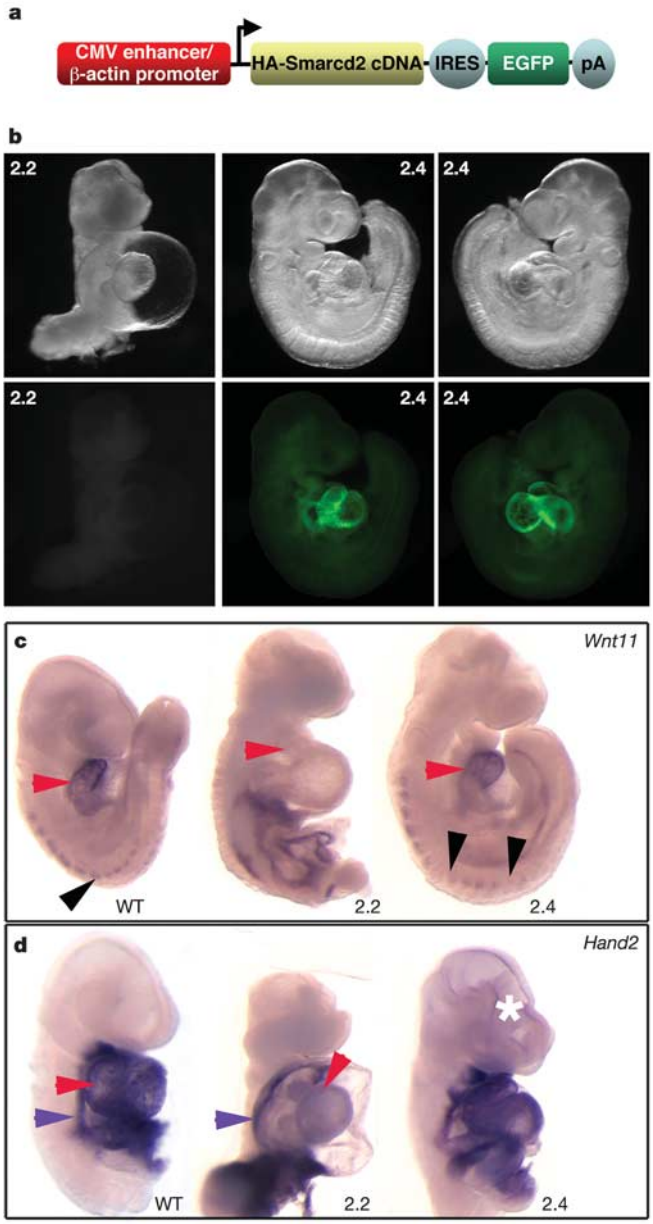

Figure 3 Transgenic rescue of heart defects in siSmarcd3 embryos. **a**, Transgenic rescue construct. HA, haemagglutinin epitope tag; IRES, internal ribosomal entry site; EGFP, enhanced green fluorescent protein; pA, polyadenylation sequence. **b**, Brightfield (top row) and EGFP fluorescence (bottom row) visualization of siSmarcd3 transgenic embryo with no transgene expression (line 2.2) and with strong cardiac-restricted transgene expression (line 2.4). Note the complete rescue of the cardiac defect in line 2.4. **c**, **d**, Expression of *Wnt11* (**c**) and *Hand2* (**d**) is reduced in line 2.2, but this is recovered in line 2.4 (transgenic rescue). Note the rescued expression of *Wnt11* in the heart (red arrowheads), but abnormal *Wnt11* expression in the somites of line 2.4 (black arrowheads), and the open neural tube in line 2.4 (asterisk in **d**). In **d**, red arrowheads show *Hand2* expression in heart; blue arrowheads show expression in lateral plate mesoderm.

To understand the basis for the cardiac defects in *Smarcd3* knockdown embryos we analysed markers of primary and anterior/secondary heart fields at the head-fold stage[6,7]. The onset of expression of cardiac transcription factor *Nkx2-5*, marking both fields, was delayed (Fig. 2a, b; Supplementary Fig. 4). However, primary and secondary heart fields were initiated normally, as shown by the expression of *Gata4*, *Isl1*, *Fgf8* and *Fgf10* (Supplementary Fig. 4, and data not shown). During chamber morphogenesis (E8.5–E9.25), overall patterning and differentiation of the heart were unaffected, as the patterned expression of *Myl2* and *Tbx5* and the expression of *Actc* and *Mybpc3* were intact (Figs 1s, t and 2g, h; Supplementary Fig. 4). Expression of *Nppa*, marking the differentiating chamber myocardium, was reduced (Fig. 2c, d). The LV marker *Hand1* was expanded (Fig. 2e, f), whereas *Hand2*, a gene essential for formation of the RV[8], was absent (Fig. 3d).

Trabecular formation was severely impaired in *Smarcd3* knockdown embryos (Fig. 1q–t). The trabeculae of the heart form as clonal outgrowths of the compact myocardium[9]. Expression of *Bmp10*, which is essential for trabecular differentiation[10], and *Irx3*, which marks trabeculae, was undetectable in *Smarcd3* knockdown embryos (Fig. 2i, j; Supplementary Fig. 4). Myocardial thickness was increased threefold (40 μm in *Smarcd3* knockdown embryos, compared with 12 μm in wild-type embryos at E9.5), indicating that cells that normally differentiate into trabeculae remained part of the myocardial wall.

Consistent with severe outflow tract defects was our observation that the expression of genes involved in outflow tract formation (*Tbx20*, *Pitx2*, *Bmp4*, *Fgf8*, *Fgf10*, *Wnt11*) was impaired (Figs 2k–p and 3c; Supplementary Fig. 4; data not shown). TdT-mediated dUTP nick end labelling staining revealed no increased apoptosis

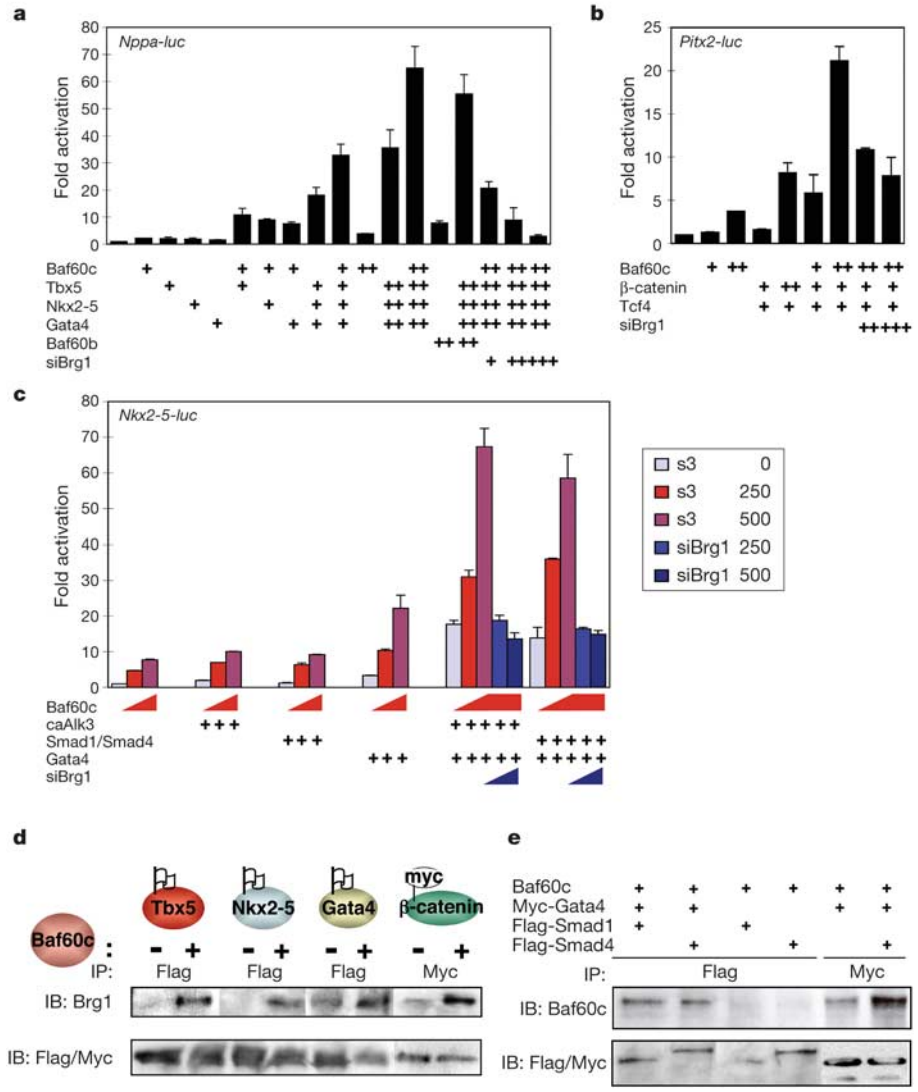

Figure 4 Baf60c potentiates transcription by promoting interactions between transcription factors and the BAF complex. **a**, Baf60c or Baf60b potentiates transactivation of *Nppa–luciferase* reporter construct by Tbx5, Nkx2-5 or Gata4, alone or in combination. **b**, Baf60c potentiates transactivation of *Pitx2-luciferase* reporter construct by activated β-catenin and Tcf4. **c**, Baf60c potentiates transactivation of *Nkx2-5-luciferase* reporter construct by Gata4 or Gata4 in combination with Smad1/Smad4 or caAlk3, but not activated BMP receptor (caAlk3) or Smad1/Smad4 alone. In **a**–**c**, one plus sign represents 50 ng of expression construct and two plus signs 100 ng, except for siBrg1. **a**–**c**, Increased transactivation by Baf60c is abrogated by siRNAs directed against *Brg1* mRNA (siBrg1; one plus sign, 100 ng; two plus signs, 250 ng; three plus signs, 500 ng). **d**, Immunoprecipitation of transfected Flag-tagged Tbx5, Nkx2-5 or Gata4, or Myc-tagged β-catenin, followed by detection of Brg1 protein shows that Brg1 can only be detected in the presence of co-transfected Baf60c, or, for Gata4 and β-catenin, the interaction with Brg1 is strengthened by Baf60c. **e**, Co-immunoprecipitation of transfected Flag-tagged Smad1 or Smad4 or Myc-tagged Gata4, co-transfected with a Baf60c expression construct, followed by detection of Baf60c protein shows that Baf60c can interact with Gata4 but not with Smad1 or Smad4. Data are presented as means and s.e.m. (error bars) for three or four independent experiments.

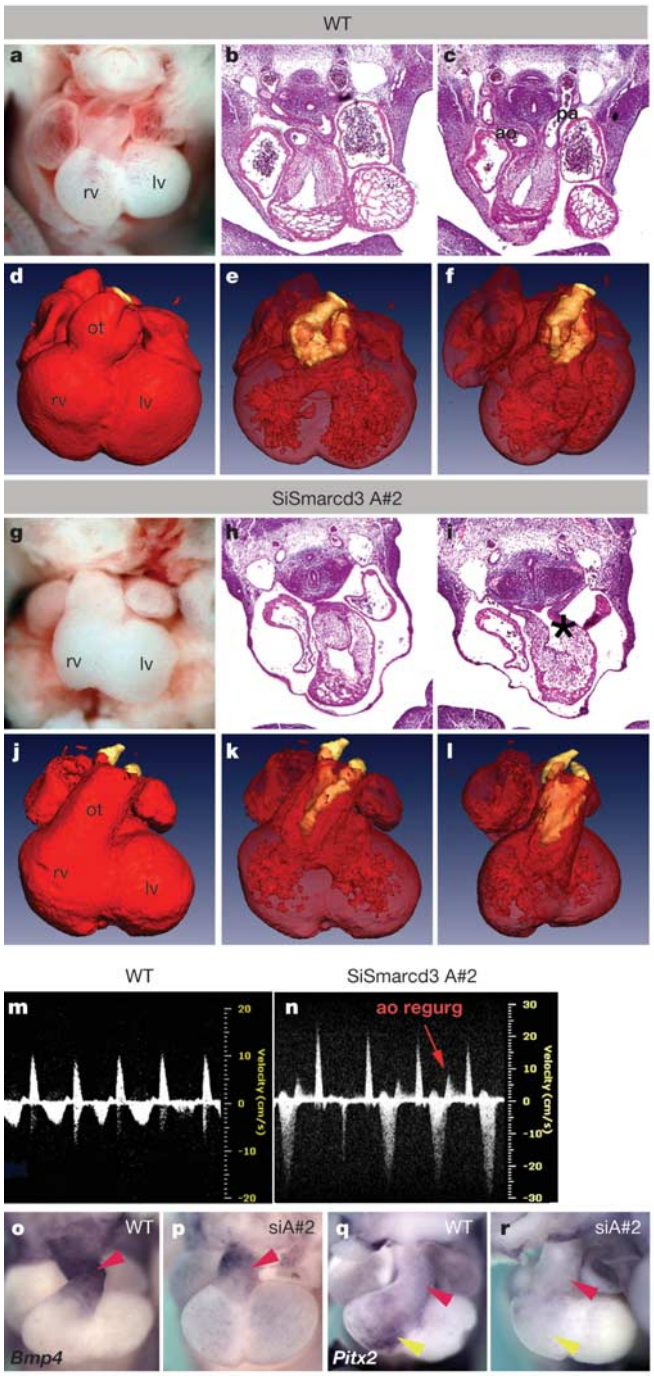

Figure 5 Dosage-sensitive role of Baf60c in outflow tract septation. **a**–**f**, Wild-type (WT) embryos at E12.5 (**a**, **d**–**f**) or E11.5 (**b**, **c**). **g**–**l**, *Smarcd3* intermediate knockdown (siSmarcd3 A#2) embryos at E12.5 (**g**, **j**–**l**) or E11.5 (**h**, **i**). WT embryos have a spiralling outflow tract, whereas siSmarcd3 A#2 embryos have a straight, unspiralled outflow tract, as shown by a brightfield view of fixed embryos (**a**, **g**), histology (**b**, **c**, **h**, **i**) and rendered OPT imaging (**d**–**f**, **j**–**l**) with the use of MF20 immunofluorescence to label cardiac muscle (red) and manually segmented PECAM immunofluorescence to label outflow tract endothelium (yellow). The opacity of the MF20 signal was decreased on the software display to permit the observation of the PECAM stain in **e**, **f**, **k** and **l**. The asterisk in **i** shows an unspiralled common outflow tract. **l**, **n**, Embryonic ultrasound demonstrates aortic regurgitation (ao regurg) in a siSmarcd2-A#2 embryo. **o**–**r**, Expression of *Bmp4* (**o**, **p**) and *Pitx2* (**q**, **r**) in wild-type (WT; **o**, **q**) and siSmarcd2-A#2 (SiA#2; **p**, **r**) embryos. ao, aorta; lv, left ventricle; pa, pulmonary artery; rv, right ventricle. Red arrows show outflow tract, yellow arrows show RV.

(data not shown), but proliferation was significantly reduced in E9.5 *Smarcd3* knockdown myocardium as assessed by immunostaining for Ki67 (Fig. 2q, r). Because outflow tract, RV and atrium arise from the anterior/secondary heart field[6,11], these results suggest that failure of expansion of the anterior/secondary heart field underlies the major cardiac defects in *Smarcd3* knockdown embryos.

Skeletal muscle differentiation relies on an interacting cascade of transcriptional activators[12]. Inhibiting the function of Brg1, the major catalytic subunit of the BAF complexes, prevents the myogenic actions of MyoD, Myf5 and MRF4 in cultured cells, and thus BAF complexes are thought to act in muscle fate determination by promoting the actions of myogenic transcription factors[13,14]. Muscle differentiation was impaired in the absence of *Smarcd3* (Supplementary Fig. 5). Although the expression of upstream myogenic genes such as *Myf5* was intact, downstream genes were not expressed, including *Mef2c*, *Myogenin* and *Actc* (Supplementary Fig. 5 and data not shown). *Actc* expression was intact in the heart, suggesting that Baf60c acts on the *Actc* muscle, but not heart, enhancer[15]. These *in vivo* results directly corroborate the proposed role for BAF complexes in promoting muscle differentiation, and show that Baf60c is a crucial mediator.

To test whether members of the Baf60 family are functionally interchangeable, we performed a transgenic rescue experiment. We used the cytomegalovirus (CMV) enhancer/chicken β-actin promoter (pCAGG), which often drives cardiac-restricted expression[16], to express Baf60b in the heart (Fig. 3a). In siSmarcd3-A#1 embryos in which cardiac-specific expression of Baf60b was achieved, heart formation and gene expression were rescued, whereas somite and neural tube defects remained (Fig. 3b–d). This demonstrates that Baf60c functions can be conferred by Baf60b, and that the RNAi-mediated phenotypes are not due to off-target effects.

Nppa, *Pitx2* and *Nkx2-5* expression was reduced in *Smarcd3* knockdown embryos. We examined the role of Baf60c in their transcriptional activation by using transient reporter assays in 10T1/2 cells. The *Nppa* promoter was activated by combinatorial interactions of Tbx5, Nkx2-5 and Gata4 (Fig. 4a)[17–19], and transfection of Baf60c or Baf60b with Tbx5, Nkx2-5 or Gata4 expression constructs individually or in combination led to synergistic activation of *Nppa–luciferase* (Fig. 4a). *Pitx2* expression in the outflow tract is regulated by Wnt signalling through Lef/Tcf binding sites[20]; activation of *Pitx2–luciferase* by activated β-catenin and Tcf4 was also potentiated by Baf60c (Fig. 4b). *Nkx2-5* expression in the cardiac crescent relies on a Smad and GATA-factor-binding element[21], and *Nkx2-5–luciferase* is strongly activated by Gata4, in synergy with bone morphogenetic protein (BMP) signalling and Smad1/Smad4 (ref. 21 and Fig. 4c). Baf60c potentiated the Gata4-dependent activation of Nkx2-5–Luc, but had minimal impact on BMP signalling and Smad1/Smad4-dependent effects, indicating that Baf60c functions by means of interactions with Gata4 but not with Smads. Inhibition of Brg1 by RNAi eliminated the synergistic activation conferred by Baf60c, showing that Baf60c depends on the presence of Brg1 (Fig. 4a–c).

To determine whether the Brg1-dependent activation conferred by Baf60c relied on direct interactions between BAF complexes and cardiac transcription factors, we transfected HeLa cells with epitope-tagged β-catenin, Tbx5, Nkx2-5 or Gata4 expression constructs, in the absence or presence of a Baf60c expression construct. Immunoprecipitation with antibodies directed against the epitope tags followed by immunoblotting for Brg1 revealed weak interactions of Brg1 with Gata4 and β-catenin as expected[22,23], and no detectable interaction with Tbx5 or Nkx2-5 (Fig. 4d). However, expression of Baf60c induced an interaction between Brg1 and both Tbx5 and Nkx2-5 and enhanced the association with Gata4 and β-catenin (Fig. 4d). Baf60c can therefore enhance interactions between transcription factors and Brg1, at least when overexpressed in cell culture. Next we examined interactions with Smads by co-immunoprecipitation and observed that Baf60c interacted with

Gata4, but not Smad1 nor Smad4 (Fig. 4e), which was consistent with our transactivation results. Because Smads recruit histone acetyltransferases (HATs) to activate transcription, we suggest a multi-step model in which BAF complexes, through interactions with Smad partners such as Gata4, synergize with HATs to allow the transition of chromatin into a transcriptionally active structure in response to transforming growth factor-β signalling[24]. We conclude that Baf60c can promote interactions between specific cardiac transcription factors and BAF complexes, thereby potentiating the activation of heart-specific genes.

Our results show that Baf60c operates during cardiac development within pathways that regulate expansion of the heart at its poles[6,7]. Baf60c interaction with Gata4 on the *Nkx2-5* cardiac crescent enhancer explains the similar cardiac defects in *Smarcd3* knockdown and *Nkx2-5*-null embryos (outflow tract defects, single ventricle and impaired trabeculation)[25,26]. An affinity of Baf60c for multiple transcription factors or specific genomic loci might provide further degrees of specificity, explaining the complex cardiac phenotype of *Smarcd3* knockdown embryos.

We used the opportunity provided by transgenic RNAi to generate an epiallelic series[5,27]. For this we used the siSmarcd3-A#2 line, which had 20% wild-type *Smarcd3* mRNA amounts in ES-cell-derived cardiomyocytes and gave rise to embryos with about 50% Baf60c protein amounts (Supplementary Fig. 3). These embryos survived until E13.0, and although overall heart formation seemed normal at E11.5, mutant hearts exhibited pericardial oedema, indicating heart failure (Fig. 5b, c, h, i). At E11.5 and E12.5 the spiralling septation of the outflow tract cushions did not occur, resulting in a straight and partly septated outflow tract (Fig. 5a–l), similar to human congenital malformations such as incomplete truncus arteriosus. We examined cardiac function *in utero* at E11.5 and found that 5 of 11 siSmarcd3-A#2 hearts had prominent outflow tract regurgitation (compared with 0 of 24 wild-type embryos), which is consistent with the outflow tract anomalies (Fig. 5m, n); siSmarcd3-A#2 embryos had lower heart rates and poorer myocardial function (Supplementary Table 1). Expression of *Pitx2* and *Bmp4*, genes important for outflow tract remodelling[20,28], was partly reduced in siSmarcd3-A#2 hearts (Fig. 5o–r), demonstrating dose-dependent gene regulation by Baf60c in the outflow tract. The phenotypes associated with the epiallelic series of reduction in *Smarcd3* mRNA amounts raise the possibility that dominant inherited congenital heart defects in humans might be caused by mutations in *Smarcd3* or other genes encoding BAF complex subunits.

Our results reveal tissue-specific and dose-dependent roles for Baf60c in recruiting BAF chromatin remodelling complexes to gene regulatory elements. Because all Baf60 isoforms are expressed in a tissue-specific manner, interactions between transcription factors and chromatin remodelling complexes might be a general feature of higher-order chromatin activation and gene regulation during tissue morphogenesis. □

Methods

In vivo RNAi and transgenesis

In vivo RNA interference was performed essentially as described in ref. 5. R1 ES cells were stably transfected with a plasmid vector containing an H1 promoter driving the expression of short hairpin RNAs (shRNAs). A neomycin resistance cassette was used for selection. Two individual shRNA sequences (siSmarcd3-A and siSmarcd3-B) were designed to distinct regions of the *Smarcd3* mRNA (see Supplementary Fig. 3). BLAST searches ensured that they were specific to *Smarcd3*. For selection of ES cells with reduced *Smarcd3* mRNA amounts, ES cells were differentiated into an enriched population of cardiac myocytes[7], and real-time reverse-transcriptase-mediated polymerase chain reaction quantified *Smarcd3* mRNA. Tetraploid aggregations were performed with knockdown ES cells to generate embryos composed entirely of transgenic ES cells[5]. Tetraploid cells expressed enhanced green fluorescent protein (EGFP), thereby ensuring that only embryos totally derived from ES cells were used in the study. Transgenic rescue was performed by transfecting line siSmarcd3-A#1 with an expression construct composed of the CMV enhancer/chicken β-actin promoter (pCAGG) driving a haemagglutinin (HA)-tagged Baf60b cDNA, followed by an internal ribosomal entry site and EGFP[16]; a puromycin resistance cassette was used for selection. Stably transfected ES cells were selected, and transgene expression was assessed by anti-HA and anti-GFP western blotting. ES cell lines with various degrees of Baf60b expression were used in tetraploid aggregations as described above. Some lines with Baf60b expression showed predominantly cardiac expression, which is characteristic of the pCAGG enhancer/promoter[16].

In situ hybridization and antibody staining

All embryos were stage-matched to controls by somite count. Whole-mount or section *in situ* hybridization was preformed in accordance with standard protocols. For fluorescent whole-mount *in situ* hybridization, embryos were hybridized with a mixture of digoxigenin-labelled *Mybpc3* and *Actc* probes, and detection was performed with rhodamine tyramide amplification reagents (Perkin-Elmer). Whole-mount immunofluorescence was done on embryos fixed in 4% paraformaldehyde, with the use of MF20 antiserum directly conjugated to Alexa 594 (Molecular Probes) and unconjugated rat anti-PECAM monoclonal antibody (Pharmingen) that was revealed with an Alexa 488-conjugated secondary antibody (Molecular Probes). The MF20 antibody developed by D. A. Fischman was obtained from the Developmental Studies Hybridoma Bank developed under the auspices of the National Institute of Child Health and Human Development and maintained by The University of Iowa (Department of Biological Sciences, Iowa City, Iowa, USA).

Optical projection tomography

Optical projection tomography (OPT) was performed essentially as described[29], on embryos fluorescently labelled by *in situ* hybridization or immunofluorescence. Visualization and manipulation of OPT data was performed with Amira software, version 3.0 (TGS Inc.). Segmentation was performed either automatically or, when necessary, manually.

Assessment of cardiac function *in utero*

Embryos in pregnant siSmarcd3-A#2 implanted mice and ICR wild-type mice were examined under isoflurane anaesthesia. An ultrasound biomicroscope (Visualsonics Inc., Toronto) with a transducer frequency of 30 MHz was used to image embryonic cardiac structures as described previously[30]. Time intervals were obtained by placing a pulsed Doppler sample volume in the common ventricle to detect inflow through the atrio-ventricular valve and outflow through the common outflow tract. At the embryonic stage of examination, no E-wave (passive filling of the ventricle during atrial relaxation) was visible. We measured isovolumetric contraction time (ICT) as the interval between the end of the A-wave (active filling of the ventricle during atrial relaxation) and the onset of the outflow wave, ejection time (ET) as the interval between the start and end of the outflow wave, isovolumetric relaxation time (IVRT) as the interval between the end of the outflow wave and the onset of the A-wave, and atrio-ventricular conduction time as the interval between the onset of the A-wave and the onset of the outflow wave. The TEI index, (ICT + IVRT)/ET, is an index of global cardiac myocardial function that is independent of heart rate and ventricular morphology.

Transactivation assays and immunoprecipitation

Transactivation assays and co-immunoprecipitation experiments were performed essentially as described in refs 17 and 18. The *Nppa–luc* and *Nkx2-5–luc* (FL construct) reporters were described previously[17,21], and the *Pitx2–luc* reporter consisted of 2.5 kb of the upstream region of the *Pitx2* translational start site (C. Meno and H. Hamada, personal communication). Anti-Brg1 (Upstate), anti-Flag (Sigma), anti-HA (Sigma), anti-Myc (Santa Cruz) and anti-GFP (Molecular Probes) antisera were obtained commercially; anti-Baf60c antiserum was provided by M.-B. Debril and J. Auwerx; anti-Baf53a, anti-Baf155 and anti-Brg1 antisera were provided by W. Wang.

Received 24 August; accepted 30 September 2004; doi:10.1038/nature03071.

1. Narlikar, G. J., Fan, H. Y. & Kingston, R. E. Cooperation between complexes that regulate chromatin structure and transcription. *Cell* **108,** 475–487 (2002).
2. Martens, J. A. & Winston, F. Recent advances in understanding chromatin remodeling by Swi/Snf complexes. *Curr. Opin. Genet. Dev.* **13,** 136–142 (2003).
3. Wang, W. *et al.* Diversity and specialization of mammalian SWI/SNF complexes. *Genes Dev.* **10,** 2117–2130 (1996).
4. Debril, M. B. *et al.* Transcription factors and nuclear receptors interact with the SWI/SNF complex through the BAF60c subunit. *J. Biol. Chem.* **279,** 16677–16686 (2004).
5. Kunath, T. *et al.* Transgenic RNA interference in ES cell-derived embryos recapitulates a genetic null phenotype. *Nature Biotechnol.* **21,** 559–561 (2003).
6. Cai, C. L. *et al.* Isl1 identifies a cardiac progenitor population that proliferates prior to differentiation and contributes a majority of cells to the heart. *Dev. Cell* **5,** 877–889 (2003).
7. von Both, I. *et al.* FoxH1 is essential for development of the anterior heart field. *Dev. Cell* **7,** 331–345 (2004).
8. Srivastava, D. *et al.* Regulation of cardiac mesodermal and neural crest development by the bHLH transcription factor, dHAND. *Nature Genet.* **16,** 154–160 (1997).
9. Meilhac, S. M. *et al.* A retrospective clonal analysis of the myocardium reveals two phases of clonal growth in the developing mouse heart. *Development* **130,** 3877–3889 (2003).
10. Chen, H. *et al.* BMP10 is essential for maintaining cardiac growth during murine cardiogenesis. *Development* **131,** 2219–2231 (2004).
11. Meilhac, S. M., Esner, M., Kelly, R. G., Nicolas, J. F. & Buckingham, M. E. The clonal origin of myocardial cells in different regions of the embryonic mouse heart. *Dev. Cell* **6,** 685–698 (2004).
12. Buckingham, M. Skeletal muscle formation in vertebrates. *Curr. Opin. Genet. Dev.* **11,** 440–448 (2001).
13. de la Serna, I. L., Carlson, K. A. & Imbalzano, A. N. Mammalian SWI/SNF complexes promote MyoD-mediated muscle differentiation. *Nature Genet.* **27,** 187–190 (2001).
14. Roy, K., de la Serna, I. L. & Imbalzano, A. N. The myogenic basic helix-loop-helix family of

transcription factors shows similar requirements for SWI/SNF chromatin remodeling enzymes during muscle differentiation in culture. *J. Biol. Chem.* **277,** 33818–33824 (2002).
15. Biben, C., Hadchouel, J., Tajbakhsh, S. & Buckingham, M. Developmental and tissue-specific regulation of the murine cardiac actin gene *in vivo* depends on distinct skeletal and cardiac muscle-specific enhancer elements in addition to the proximal promoter. *Dev. Biol.* **173,** 200–212 (1996).
16. Toyoda, M. *et al.* jumonji downregulates cardiac cell proliferation by repressing cyclin D1 expression. *Dev. Cell* **5,** 85–97 (2003).
17. Durocher, D., Charron, F., Warren, R., Schwartz, R. J. & Nemer, M. The cardiac transcription factors Nkx2-5 and GATA-4 are mutual cofactors. *EMBO J.* **16,** 5687–5696 (1997).
18. Bruneau, B. G. *et al.* A murine model of Holt–Oram syndrome defines roles of the T-box transcription factor Tbx5 in cardiogenesis and disease. *Cell* **106,** 709–721 (2001).
19. Garg, V. *et al.* GATA4 mutations cause human congenital heart defects and reveal an interaction with TBX5. *Nature* **424,** 443–447 (2003).
20. Kioussi, C. *et al.* Identification of a Wnt/Dvl/β-catenin → Pitx2 pathway mediating cell-type-specific proliferation during development. *Cell* **111,** 673–685 (2002).
21. Brown, C. O. *et al.* The cardiac determination factor, Nkx2-5, is activated by mutual cofactors GATA-4 and Smad1/4 via a novel upstream enhancer. *J. Biol. Chem.* **279,** 10659–10669 (2004).
22. Kadam, S. & Emerson, B. M. Transcriptional specificity of human SWI/SNF BRG1 and BRM chromatin remodeling complexes. *Mol. Cell* **11,** 377–389 (2003).
23. Barker, N. *et al.* The chromatin remodelling factor Brg-1 interacts with β-catenin to promote target gene activation. *EMBO J.* **20,** 4935–4943 (2001).
24. Derynck, R. & Zhang, Y. E. Smad-dependent and Smad-independent pathways in TGF-β family signalling. *Nature* **425,** 577–584 (2003).
25. Lyons, I. *et al.* Myogenic and morphogenetic defects in the heart tubes of murine embryos lacking the homeo box gene Nkx2-5. *Genes Dev.* **9,** 1654–1666 (1995).
26. Tanaka, M., Chen, Z., Bartunkova, M., Yamazaki, N. & Izumo, S. The cardiac homeobox gene Csx/Nkx2.5 lies genetically upstream of multiple genes essential for heart development. *Development* **126,** 1269–1280 (1999).
27. Hemann, M. T. *et al.* An epi-allelic series of p53 hypomorphs created by stable RNAi produces distinct tumor phenotypes *in vivo*. *Nature Genet.* **33,** 396–400 (2003).
28. Liu, W. *et al.* Bmp4 signaling is required for outflow-tract septation and branchial-arch artery remodeling. *Proc. Natl Acad. Sci. USA* **101,** 4489–4494 (2004).
29. Sharpe, J. *et al.* Optical projection tomography as a tool for 3D microscopy and gene expression studies. *Science* **296,** 541–545 (2002).
30. Zhou, Y. Q. *et al.* Applications for multifrequency ultrasound biomicroscopy in mice from implantation to adulthood. *Physiol. Genomics* **10,** 113–126 (2002).

Supplementary Information accompanies the paper on **www.nature.com/nature**.

Acknowledgements We thank J. Sharpe for providing a prototype OPT system, S. McMaster for tetraploid aggregations, D. Holmyard for scanning electron microscopy, K. Harpal and K. Koshiba-Takeuchi for histology, H. Hamada and C. Meno for the unpublished *Pitx2* reporter, and A. Nagafuchi, M. Nemer, R. Schwartz, D. Srivastava and T. Takeuchi for reporter and expression constructs. This research was funded by the Canadian Institutes of Health Research (CIHR; to B.G.B., J.R. and J.L.W.), the Heart and Stroke Foundation of Ontario (to B.G.B.), the March of Dimes Birth Defects Foundation (to B.G.B.), NCIC (to J.L.W.), the Canada Foundation for Innovation (to R.M.H.), an Emmy–Noether fellowship of the Deutsche Forschungsgemeinschaft (to H.L.), a Human Frontiers Science Program long-term fellowship (to J.K.T.), an OGSST fellowship (to J.R.W.), and the Koeln Fortune Program, University of Cologne (to I.v.B.).

Competing interests statement The authors declare that they have no competing financial interests.

Correspondence and requests for materials should be addressed to B.G.B. (bbruneau@sickkids.ca) or J.R. (rossant@mshri.on.ca).

A *faux* 3′-UTR promotes aberrant termination and triggers nonsense-mediated mRNA decay

Nadia Amrani, Robin Ganesan, Stephanie Kervestin, David A. Mangus, Shubhendu Ghosh & Allan Jacobson

Department of Molecular Genetics and Microbiology, University of Massachusetts Medical School, Worcester, Massachusetts 01655-0122, USA

Nonsense-mediated messenger RNA decay (NMD) is triggered by premature translation termination[1–3], but the features distinguishing premature from normal termination are unknown. One model for NMD suggests that decay-inducing factors bound to mRNAs during early processing events are routinely removed by elongating ribosomes but remain associated with mRNAs when termination is premature, triggering rapid turnover[4]. Recent experiments[5–7] challenge this notion and suggest a model that posits that mRNA decay is activated by the intrinsically aberrant nature of premature termination[8,9]. Here we use a primer extension inhibition (toeprinting) assay[10] to delineate ribosome positioning and find that premature translation termination in yeast extracts is indeed aberrant. Ribosomes encountering premature UAA or UGA codons in the *CAN1* mRNA fail to release and, instead, migrate to upstream AUGs. This anomaly depends on prior nonsense codon recognition and is eliminated in extracts derived from cells lacking the principal NMD factor, Upf1p, or by flanking the nonsense codon with a normal 3′-untranslated region (UTR). Tethered poly(A)-binding protein (Pab1p), used as a mimic of a normal 3′-UTR, recruits the termination factor Sup35p (eRF3) and stabilizes nonsense-containing mRNAs. These findings indicate that efficient termination and mRNA stability are dependent on a properly configured 3′-UTR.

The yeast *can1-100* allele contains a premature UAA codon at position 47 of the *CAN1* coding region that effectively terminates translation and destabilizes the *CAN1* mRNA[11]. We constructed a gene that fused the UAA-containing segment of *can1-100* to the firefly *LUC* coding region, and used this construct to generate synthetic mRNA (UAA RNA). We also created a variant with a weak terminator (CAA UGA CAA)[12] at codon 47 (UGA RNA) and two control RNAs with no early stop codon (Fusion and AAA RNAs; Fig. 1a). *In vivo*, the UAA and UGA RNAs were substrates for NMD. All of these mRNAs were incubated in translation reactions with wild-type extracts and subjected to toeprinting analyses, using sensitivity to the cap analogue ^{7}mGpppG, an inhibitor of translation initiation, as a method of distinguishing genuine toeprints from background bands[10]. Toeprints corresponding to ribosomes stalled with a stop codon in their A sites were obtained with the UAA and UGA RNAs at the expected position 12–14 nucleotides (nt) downstream of the premature nonsense codons[10] (Fig. 1b, lanes 1 and 3). The toeprints were dependent on translation because they were sensitive to cap analogue (lanes 2 and 4), and were dependent on the presence of a stop codon (which is absent from the Fusion RNA; lanes 5 and 6). Similar experiments failed to detect any toeprint signals from the normal UAA termination codons of either Fusion or *ADE2* RNAs, even after long periods of translation (Supplementary Fig. 1a) or incubation in extracts with the temperature-sensitive termination factor Sup45p/eRF1 (data not shown). These results indicate that ribosomes that terminate prematurely are released much less efficiently than those encountering normal terminators.

Addition of the elongation inhibitor cycloheximide to the translation reactions also failed to reveal toeprints from normal terminators (data not shown) but did allow the detection of additional toeprints[13,14]. Cycloheximide-dependent initiator AUG toeprints on the UAA, UGA, Fusion and AAA RNAs were sensitive to cap analogue (Fig. 1c, top arrow, lanes 1–6; Fig. 1d, top) and reflect 80S ribosomes, centred on AUG codons, protecting 16–18 nt 3′ to those codons. Other cycloheximide-dependent toeprints were present in close proximity to the locations of the early stop codons. These unexpected bands mapped to a position 6–7 nt downstream of the terminator U in both the UAA and UGA RNAs (Fig. 1c, lanes 1 and 3, middle arrow), as well as to a position 17 nt downstream of the terminator U in the UGA RNA (lane 3, bottom arrow). The appearance of these toeprints was dependent on concurrent mRNA translation (lanes 2 and 4), the presence of yeast extract (lanes 7–9), and recognition of a termination codon (lanes 5 and 6; Fig. 1d, bottom). The dependence of these toeprints on prior termination codon recognition was underscored by experiments showing that, after the addition of cycloheximide, the +6 toeprint of the UAA RNA accumulated after the disappearance of the +12 toeprint